A FACILE SYNTHESIS OF AMORPHOUS SILICA NANOPARTICLES BY SIMPLE THERMAL TREATMENT ROUTE

I. M. ALIBE[a,c], K. A. MATORI[a,b*], E. SAION[b], A. M. ALIBE[d,e], M. H. M. ZAID[b], E. A. A. GHAPUR ENGKU[a]

[a]*Institute of Advanced Technology, Universiti Putra Malaysia, 43400 UPM Serdang, Selangor, Malaysia*
[b]*Departments of Physics, Faculty of Science, Universiti Putra Malaysia, 43400 UPM Serdang, Selangor, Malaysia*
[c]*National Research Institute for Chemical Technology Zaria, Kaduna State Nigeria*
[d]*Mechanical Engineering Departments, Federal Polytechnique Damaturu Yobe, State Nigeria*
[e]*Departments of Mechanical, Automotive and Manufacturing, Faculty of Engineering and Computing, Coventry University, CV1 5FB, Coventry, United Kingdom*

A facile thermal treatment route was for the first time used to successfully synthesize amorphous silica nanoparticles. Various techniques were employed to study the structural, phase and elemental composition of the material at different calcination temperature between 500–750°C. The XRD analysis confirms the formation silica to be in an amorphous state and further revealed that the material remained in amorphous state even when calcined at 750°C. The FT–IR spectra shows that the calcination process has enable the removal of organic source from PVP and formation of amorphous silica nanoparticles. The average particle size of the material estimated from the TEM images shows that the particle were <10nm. The optical absorbance exhibited in the UV region reveals amorphous silica nanoparticles possess a wide band gap ranging from 3.803– 4.126 eV calcined between 500 to 750 °C. The EDX analysis has confirmed the presence of Si and O as the only elements in the material formed, which implies thermal treatment method is effective for the synthesis of amorphous silica nanoparticles.

1. Introduction

Nanotechnology is multi-disciplinary specialization which cut across the conventional boundaries between physics, chemistry, mathematics, biology and engineering [1]. With these ideas, the technologist and engineer maneuver materials at nanoscale to create a product which make use of remarkable properties. In nanomaterial research and development, synthesis and characterization plays an important role. Top-down and bottom-up approach technique, are the two major approaches for nanomaterials assembling. In top-down method, nanomaterials are constructed from large size material without molecule level control [2]. While the bottom-up approach, is where materials are constructed from a few molecule components by chemical self-assembling in solution into functional superstructure. The development of ceramic nanomaterial with improved structural and optical properties has been studied with much success in recent years. Such as silica, alumina, titania, zirconia, silicon nitride and silicon carbide.

Amorphous silica nanoparticles (ASN) occupy a prominent position in scientific research, because of their easy preparation and their wide uses in various industrial applications, such as catalysis, pigments, pharmacy, electronic and thin film substrates, electronic and thermal insulators, and humidity sensors [3, 4].

Several procedures and methods have been reported on the synthesis of ASN with the aim of its improving the chemical and physical features. Such methods include sol-gel technique [5], spray pyrolysis [6], hydrothermal growth [7] and micro wave assisted method [8]. However, most of these methods are difficult to apply on large scale production due to the complicated procedure, high temperature involved, and longer period of reaction, toxic chemical reagent and harmful by product release to the environment at the end of the experiments [9].

The present study synthesized ASN by simple thermal treatment method from an aqueous solution containing silicon tetraacetate, PVP Poly (vinyl pyrrolidone) and deionizes water only [9, 10]. The influence of calcination temperature on the structural and optical property have been studied and discussed in details.

2. Experimental

2.1 Materials

Silicon tetraacetate reagent $Si(OCOCH_3)_4$(M_w = 264.26 g/mol), was purchased from sigma Aldrich and used as metallic precursors, poly(vinyl pyrrolidone) (PVP M_w = 29000 g/mol) was also purchased from sigma Aldrich which served as capping agent, hence reduce agglomeration and stabilize the nanoparticles. Deionized water served as solvent. All chemicals used were more than 99% purity and used without any further purification

2.2 Procedure

A solution of PVP was made by dissolving 3 g of PVP in 100 ml of deionized water and continuously stirred using magnetic stirrer for 2h, until no precipitate formed. Later 0.2 mmol of $Si(OCOCH_3)_4$was added and stirred continuously for another 2 h, little. The solution was transferred into a clean petri dish and dried in an oven for 24 h at 80 ^{o}C. The resulting solid gel was grinded in a sterilized mortal into powder form. The powder was placed into crucible boat and calcinated in a box furnace at 500 ^{o}C, 550 ^{o}C, 600 ^{o}C, 650 ^{o}C, 700 ^{o}C, and 750 ^{o}C, with constant holding time 3 h to decompose PVP and produce ASN.

2.3 Characterization

The synthesized ASN were characterized by several techniques such as, FT-IR, EDX, XRD, TEM, FESEM and UV-vis. The precursor before calcination was characterized by TGA analysis. The bond formation and functional group of ASN has been studied by infrared spectra (FT-IR Perkin Elmer model 1650). The structural behaviour of the ASN was examine by X-ray diffraction (XRD Shimadzu model 6000 using Cu kα (0.154 nm) as a radiation source to generate diffraction patterns from the sample at ambient temperature in 2θ within the range of 20-80°. The elemental composition was examined using Field electron scanning microscopy (FESEM) (JEOL JSM-7600F) equipped with EDX. The particle size and distribution were examine by Transmission electron microscopy (TEM) (JEOL TEM model 2010F UHR) with an accelerating voltage of 200 kN. The optical properties were determined by UV-vis spectrometer (Shimadzu model UV-3600) at room temperature in the range of 200-800 nm.

3. Results and Discussion

3.1 Thermogravimetric Analysis (TGA-DTG)

TGA analysis for the removal or decomposition of poly (vinyl pyrrolidone) (PVP) are both shown in Figure 1. The graph was plotted for weight loss percentage as a function of temperature of the dried sample prior to calcination process. The sample exhibited two different steps of decomposition. The first one was weight loss due to the moisture already entrapped in sample at temperature of 83 °C. In 2014, Al Hada et al. [9] reported that the moisture entrapped in the PVP could be removed at 84 °C. The other stage of weight loss was observed at 437 °C which implies that most of the PVP has given off. There was no considerable weight losses observed as the

temperature approached 486 °C. At that instance, there was complete decomposition of PVP, thus leaving behind only a residue of SiO_2.
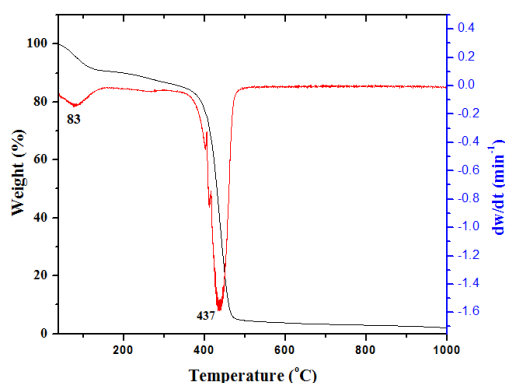
Fig. 1: The thermogravimetry (TG) and thermogravimetry derivative (DTG) curves
for PVP used to determine the minimum calcination temperature
at heating rate of 10 °C /min.

3.2 Phase and Elemental Composition Analysis

The elemental analysis of SiO_2 was tested by Energy-dispersive X-ray spectroscopy (EDX). The basic principle is such that every particular element possesses a unique atomic structure allowing particular set of peaks on its X-ray spectrum.

The purpose of carrying out the EDX analysis here was to enable confirm the elemental composition of the constituent atoms and figure out if there are any foreign impurity atoms. Figure 2 shows the EDX spectrum of SiO_2 calcined at 500°C. The corresponding peaks of Si, and O_2 were observed in the sample which confirms the formation of pure SiO_2 and further confirmed the results obtained from XRD analysis. In conclusion, the EDX analysis confirms the formation of SiO_2 and also proves that the thermal treatment technique is effective, as there were no loss of element was observed in the process.
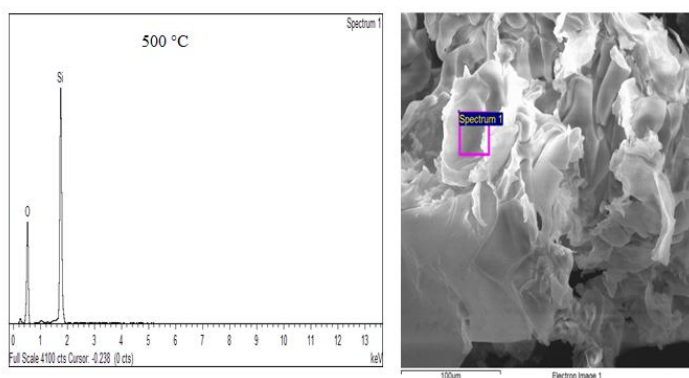
Fig. 2: EDX pattern of ASN for sample calcined at 500 °C

The FT-IR offers vital evidence on the vibrational frequencies of functional groups and network structures of a certain material. A certain vibration frequency range can be ascribed to a bond type, as specific frequencies are absorbed by the molecules of the materials which are characteristic of their structure. Frequency of the absorbed radiation is attributed to the frequency of the bond or group that vibrates. In this work, the ASN were examined for the interface between the formation of the compound and the polymer (PVP) matrix at different calcination temperatures by the FT-IR.

The analysis of the precursor at room temperature before calcination was conducted, to observe the organic and inorganic behaviour of the material prior to calcination, as well as after calcination. The analysis was conducted within the range of 280-400 cm^{-1} as being shown by the FTIR spectra in Figure 3, and Table 1 respectively.
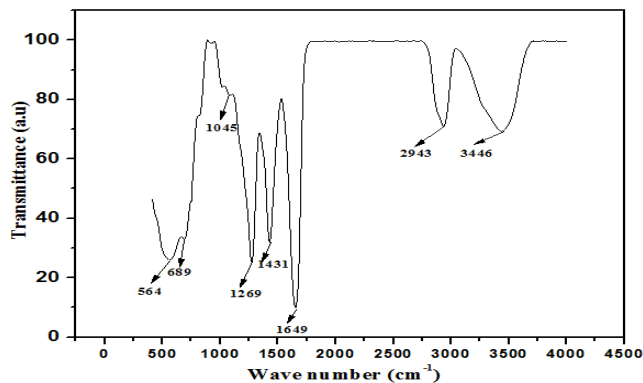
Fig. 3: FT-IR spectra of ASN precursor before calcinations

The availability of peaks in the precursor before calcination shown in Figure 3, beyond 1000 cm^{-1} indicates the existence of organic source coming from the PVP. The C-N stretching vibration peak was observed at 1269 cm^{-1}. The peak appeared at 1431 cm^{-1} was attributed to C-H bending vibrations originated from methylene group. The band at 1649 cm^{-1} was due to N-H stretching vibration and the two different bands at 2951 cm^{-1} and 3457 cm^{-1} observed was assigned to C-H stretching and N-H stretching vibration respectively. The peak 1045 cm^{-1} was observed to be OH group Si-O bending vibration and Si-O bond vibration was observed at 564 and 689 cm^{-1} respectively.

The FT-IR spectra of reveals the removal PVP and the effect of the calcination temperature on bond formation of ASN as shown in Figure 4. The Si-O-Si bending vibration was observed at 445 cm^{-1} for the sample calcined at 500-700 °C and shifted to higher wave number of 457 cm^{-1} when calcine at 750 °C. There were no shifts of peak at 798 cm^{-1} due to Si-O-Si bond observed in all the samples calcined. An asymmetric vibration mode of Si-O-Si was exhibited at 1062 cm^{-1} at all calcination temperature [3, 11]. Band due to water molecules and OH in H-bonded water where observed respectively between 500-600 °C. The FT-IR analysis revealed the bonds related to SiO$_2$ and further confirm the formation of SiO$_2$ as shown in the EDX result.
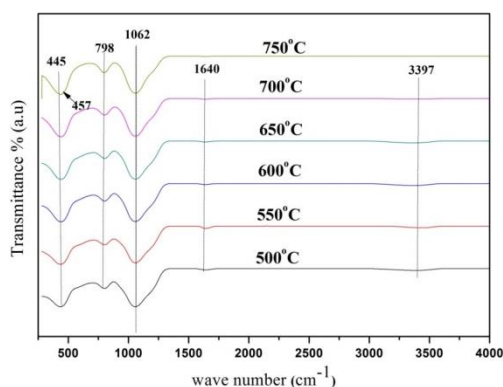
Fig. 4: FT-IR spectra of ASN calcined at various temperatures in the range of 280-4500 cm^{-1}

3.3 The Structural Analysis

The phase and structure of the material was observed by analyzing the sample using X-ray diffraction spectroscopy. The main precursor that contain silicon tetraacetate and PVP after being dried at 80 °C shows no diffraction peaks indicating that the sample was amorphous at room temperature before calcination as shown in Fig. 5
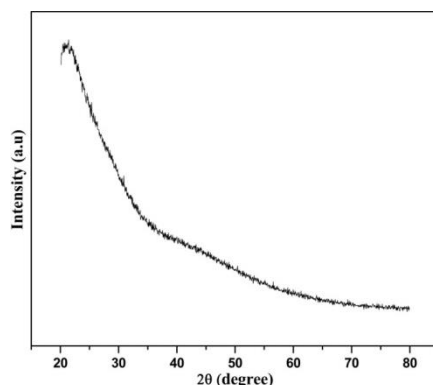
Fig. 5: XRD patterns for SiO$_2$ precursor before calcination at room temperatures

Upon calcination of the sample between 500-700°C as shown in Figure 6, the samples behave to be in amorphous state (ASN), as there were no significant peaks. In 2014, Rida and Harb[12] reported to have produced ASN at the calcination temperature of 650 °C. In the same vain, an amorphous cobalt doped SiO$_2$ was synthesized between 300-500°C [13]. Nevertheless, in 2014, Musić et al. [14] could not produce crystal phase of SiO$_2$ at 800 °C until the temperature was elevated to 1000 °C. However, in this work, a peak was observed after calcination at 750 °C at a position of 2θ=26.56°. The spectrum corresponds to Cristobalite beta high with ICDS collection code 77401.
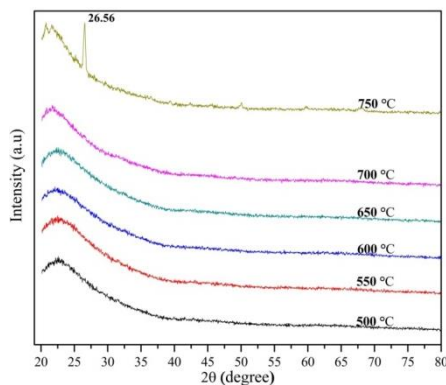
Fig. 6: XRD patterns for ASN calcined at temperatures 500, 550, 600, 650, 700 and 750°C.

3.4 Morphology and Particle Size Distribution

TEM analysis was used to examine the influence of the calcination temperature ranging from 500-750 °C on the shape, size as well as particles distribution of the prepared ASN. The TEM images were obtained using Model JOEL 2010F UHR version electron microscope at accelerating voltage of 200 kV. The same procedures were followed in determining the distribution of the particles and average size of the nanoparticles using image J software
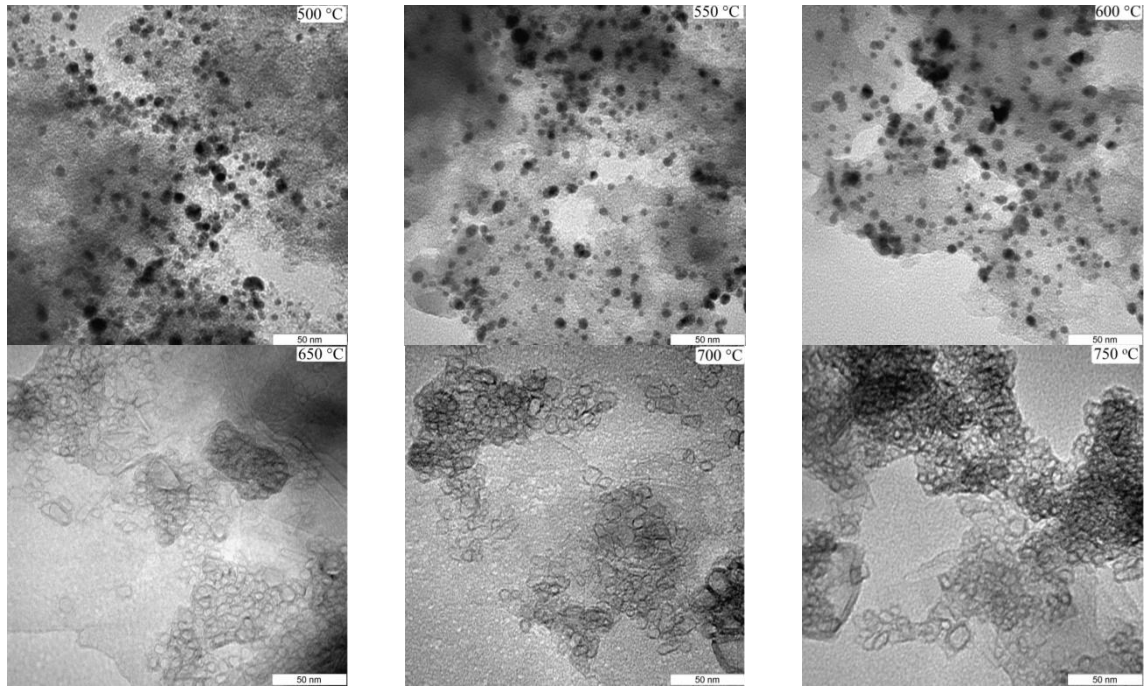
*Fig. 7: TEM images of ASN calcined
at 500, 550, 600, 650, 700 and 750 °C.*
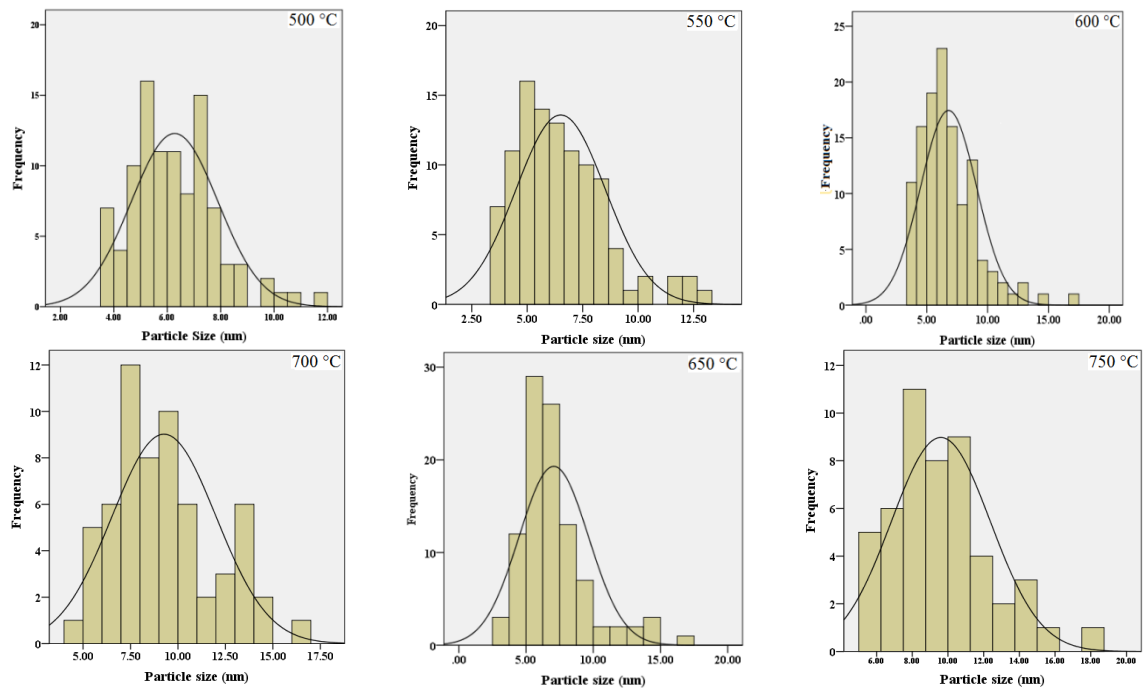
*Fig. 7: TEM images and particle size distribution of ASN calcined
at 500, 550, 600, 650, 700 and 750 °C.*

In this work, the particles size of ASN ranges from 6.28 nm to 9.60 nm as the temperature varies from 500 to 750 °C shown in Table 2 and Fig 7. The images seems to be <10 nm at the entire calcination temperatures and obtained the smallest particle size at the temperature of 500 °C and the particles size reluctantly increases with the increasing in temperature. This implies that

thermal treatment method was for the first time used to prepare amorphous silica nanoparticles with less than 10 nm particle size.

3.5 Optical Properties

The absorbance behavior of ASN was studied using UV-visible spectrophotometer. The samples were calcinated between 500-750°C as shown in Figure 8. The entire sample calcined exhibits an optical absorbance in the UV region which implies that they possess a wide band gap as reported in the literature [15, 16]. The peaks at 243 nm which appeared in all the sample was famous in silica nanoparticles reported by some literatures to as singlet to singlet transition in silicon related intrinsic defect [17, 18]. The peaks between 300-320 nm were attributed to various defects due to non-bridging oxygen hole centre or neutral oxygen vacancies (ODCs) defects [17].
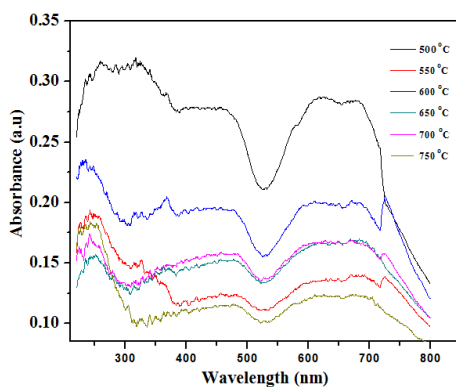
Fig. 8: Absorbance spectra of ASN calcine at various temperatures

3.6 Band gap energy of ASN

The influence of the calcination temperature was observed on the optical band gap of the entire sample as shown in Figure 9 which was determined from the absorption coefficient value. The energy gap (Eg) is considered as reported assuming a direct transition between valence and conduction bands [19]. The relation is given by the expression (1) below.

$$(\propto h\upsilon)^2 = A(h\upsilon - Eg) \tag{1}$$

Where A is a constant, the photon energy is denoted by $h\upsilon$ and Eg is the optical energy band. As shown in Figure 9 we have plotted the characteristics $(\propto h\upsilon)^2$ versus $h\upsilon$ values, where the optical band gap of the material was determined by simply extrapolating the linear region to where $(\propto h\upsilon)^2$ tends to zero.
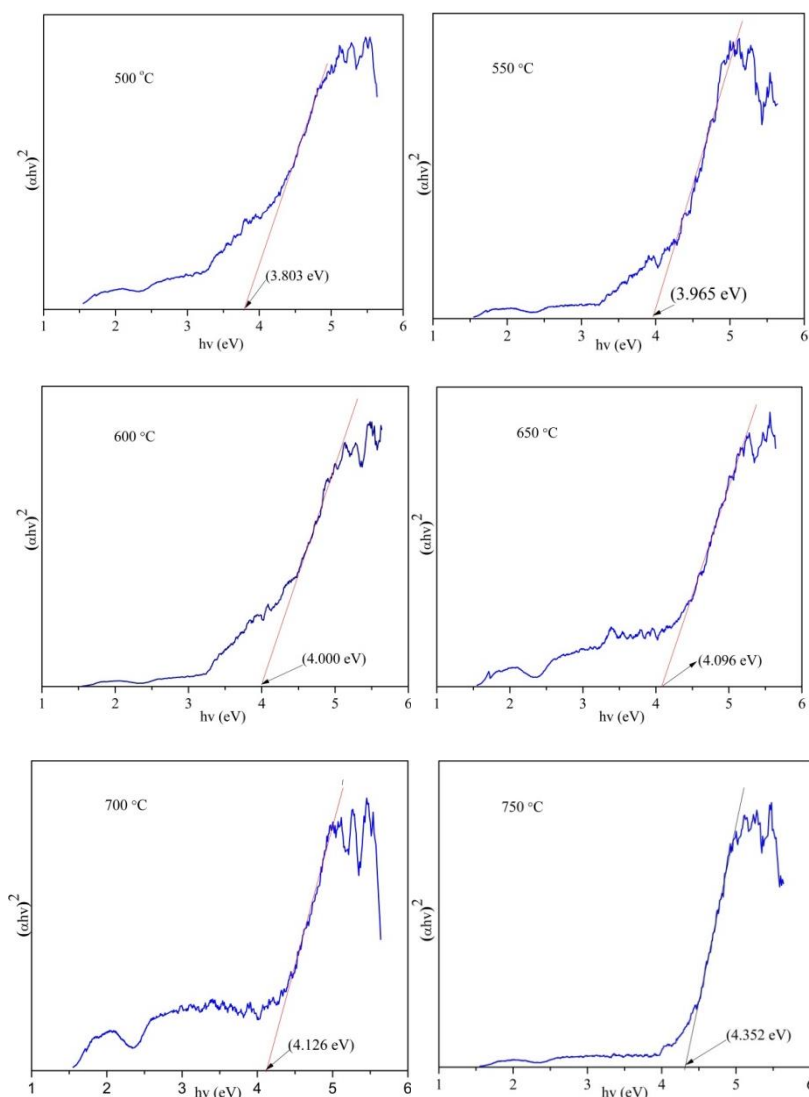
Fig. 9: Plot of the $(\propto h\upsilon)^2$ as function of photon energy of ASN calcined at various temperatures

Table 2: The average particle size of ASN measured by TEM and comparison of the band gap energy for samples calcined at various temperatures

Temperature (°C)	D_{TEM} (nm)	Eg (eV)
500	6.28	3.803
550	6.51	3.965
600	6.80	4.000
650	7.06	4.096
700	9.26	4.126
750	9.60	4.352

The optical band gap was found to be 3.803, 3.965, 4.000, 4.096, 4.126 and 4.352 eV respectively as the calcination temperature was increase from 500 to 750°C. Figure 10 gives the relationship between the optical bandgap and the calcination temperature.
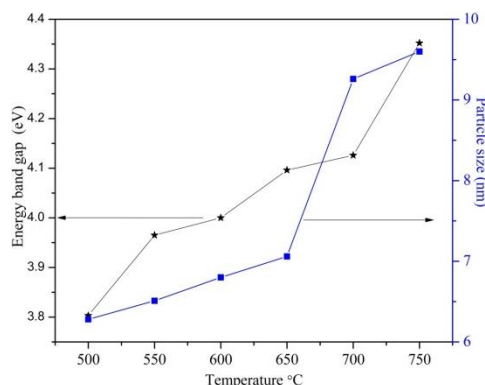
Fig. 10: A graph showing the influence of calcination temperature on the particles size and optical band gap ASN.

4. Conclusions

A simple thermal treatment method was successfully applied to synthesize ASN. The FT-IR confirmed the bond formation after calcination which reveals the presence of SiO_2 bond and also completes the disappearance of PVP in the sample. The XRD result reveals the sample to be ASN at all calcination. A wide band gap energy observed in the material was attributed to the absorption exhibited in the UV region.

Acknowledgments

References

[1] O. V. Salata, Journal of nanobiotechnology, **2,** 1 (2004).

[2] T. S, Wong, B, Brough, C. M. Ho, Molecular and Cellular Biomechanics: MCB, **6**, 1-55 (2009).

[3] M. A, Akl, H. F, Aly, H. M. A, Soliman, M. E, Aref,A. ElRahman,. J NanomedNanotechnol, **4**, 183(2013).

[4] G, Cho, J, Jang, S, Jung, I. S, Moon, J. S, Lee, Y. S, Cho, E. A, O'Rear, Langmuir, **18**, 3430 (2002).

[5] L. P, Singh, S. K, Bhattacharyya, R, Kumar, G, Mishra, U, Sharma, G, Singh, S. Ahalawat, Advances in colloid and interface science, **214**, 17-37 (2014).

[6] K, Okuyama, I. W, Lenggoro, Chemical Engineering Science, **58**(3), 537 (2003).

[7] H, Song, R. M, Rioux, J. D, Hoefelmeyer, R, Komor, K, Niesz, M, Grass, G. A, Somorjai, Journal of the American Chemical Society, **128**, 3027 (2006).

[8] Y, Sha, C, Deng, B, Liu, Journal of Chromatography A,**1198**, 27 (2008).

[9] N. M. Al-Hada, E. B. Saion, A. H. Shaari, M. A. Kamarudin, M. H. Flaifel, S. H. Ahmad, S. A. Gene, PloS one, **9,** 8 (2014).

[10] M, Goodarz Naseri, E. B, Saion, A, Kamali, An overview on nanocrystalline $ZnFe_2O_4$, $MnFe_2O_4$, and $CoFe_2O_4$ synthesized by a thermal treatment method. ISRN Nanotechnology, doi:10.5402/2012/604241 2012.

[11] A, Beganskiene, V, Sirutkaitis, M, Kurtinaitiene, R, Juskėnas, A, Kareiva,. Materials Science (Medziagotyra), **10**, 287 (2004).

1164

[12] M. A, Rida,F. Harb. Journal of Metals, Materials and Minerals, **24**, 37 (2014).

[13] J, Liu, X, Wei, X, Wang, and X.-W, Liu, Chemical Communications, **47,** 6135 (2011).

[14] S, Music, N, Filipović-Vincekovic,L, Sekovanic, Brazilian Journal of Chemical Engineering, **28**, 89 (2011).

[15] T. López, M. Alvarez, S. Arroyo, A. Sánchez, D. Rembao, Journal of Biotechnology and Biomaterial **S4:001**, doi:10.4172/2155-952X.S4-001. (2011)

[16] R, Nandanwar, P, Singh, F. Z, Haque,. American Chemical Science Journal, **5** 1 (2015).

[17] M, Jafarzadeh, I. A, Rahman, C. S, Sipaut, Ceramics International, **36**, 333 (2010).

[18] L. N, Skuja, A. N, Streletsky, A. B, Pakovich, Solid State Communications, **50**, 1069 (1984).

[19] N, Kenny, C. R, Kannewurf, D. H, Whitmore Journal of Physics and Chemistry of Solids, **27**, 1237 (1966).